[CANCER RESEARCH 64, 2120–2126, March 15, 2004]

Choice of Oxygen-Conserving Treatment Regimen Determines the Inflammatory Response and Outcome of Photodynamic Therapy of Tumors

Barbara W. Henderson,[1] Sandra O. Gollnick,[1] John W. Snyder,[1] Theresa M. Busch,[4] Philaretos C. Kousis,[1] Richard T. Cheney,[2] and Janet Morgan[3]

[1]Department of Cellular Stress Biology and the Photodynamic Therapy Center, [2]Department of Pathology and Lab Medicine, and [3]Department of Dermatology, Roswell Park Cancer Institute, Buffalo, New York, and [4]Department of Radiation Oncology, University of Pennsylvania, Philadelphia, Pennsylvania

ABSTRACT

The rate of light delivery (fluence rate) plays a critical role in photodynamic therapy (PDT) through its control of tumor oxygenation. This study tests the hypothesis that fluence rate also influences the inflammatory responses associated with PDT. PDT regimens of two different fluences (48 and 128 J/cm^2) were designed for the Colo 26 murine tumor that either conserved or depleted tissue oxygen during PDT using two fluence rates (14 and 112 mW/cm^2). Tumor oxygenation, extent and regional distribution of tumor damage, and vascular damage were correlated with induction of inflammation as measured by interleukin 6, macrophage inflammatory protein 1 and 2 expression, presence of inflammatory cells, and treatment outcome. Oxygen-conserving low fluence rate PDT of 14 mW/cm^2 at a fluence of 128 J/cm^2 yielded ~70–80% tumor cures, whereas the same fluence at the oxygen-depleting fluence rate of 112 mW/cm^2 yielded ~10–15% tumor cures. Low fluence rate induced higher levels of apoptosis than high fluence rate PDT as indicated by caspase-3 activity and terminal deoxynucleotidyl transferase-mediated nick end labeling analysis. The latter revealed PDT-protected tumor regions distant from vessels in the high fluence rate conditions, confirming regional tumor hypoxia shown by 2-(2-nitroimidazol-1[*H*]-yl)-N-(3,3,3-trifluoropropyl) acetamide staining. High fluence at a low fluence rate led to ablation of CD31-stained endothelium, whereas the same fluence at a high fluence rate maintained vessel endothelium. The highest levels of inflammatory cytokines and chemokines and neutrophilic infiltrates were measured with 48 J/cm^2 delivered at 14 mW/cm^2 (~10–20% cures). The optimally curative PDT regimen (128 J/cm^2 at 14 mW/cm^2) produced minimal inflammation. Depletion of neutrophils did not significantly change the high cure rates of that regimen but abolished curability in the maximally inflammatory regimen. The data show that a strong inflammatory response can contribute substantially to local tumor control when the PDT regimen is suboptimal. Local inflammation is not a critical factor for tumor control under optimal PDT treatment conditions.

INTRODUCTION

Photodynamic therapy (PDT), which uses the activation of tumor-localizing photosensitizing agents by visible light, is an effective therapy for local malignant tumors, achieving palliation of advanced disease and cure of early disease (1, 2). Its mechanism of action is the local generation of cytotoxic singlet oxygen ($^1O_2$), which results in damage to tumor cells and stroma, especially the tumor vasculature, and usually is accompanied by an inflammatory response.

Because $^1O_2$ originates from energy transfer from the excited photosensitizer to ground-state oxygen, thereby consuming oxygen, PDT critically depends on tissue oxygen levels. The light fluence rate (irradiance) has been identified as a major factor determining tumor oxygen levels during PDT (3–6). High fluence rates may lead to high rates of $^1O_2$ generation and thus oxygen consumption, which may outpace the rate of oxygen diffusion from the capillaries. This shrinks the volume of oxygenated and therefore PDT-sensitive tumor tissue, resulting in decreased treatment efficacy; conversely, low fluence rates may maintain tumor oxygenation and enhance PDT efficacy (7, 8).

Inflammation has been assigned an important role among the mechanisms influencing tumor control by PDT and is considered an important priming event for the development of specific antitumor immunity (1, 9). It has been studied in a number of tumor models and with several photosensitizers (10–13). PDT-induced inflammatory changes are characterized by enhanced expression of a number of proinflammatory cytokines and chemokines, including interleukin 1β (IL-1β), tumor necrosis factor α (TNF-α), IL-6, and macrophage inflammatory proteins 1 and 2 (MIP-1 and MIP-2), and adhesion molecules E-selectin and intercellular adhesion molecule (12–16). Marked leukocyte infiltration into the treated tumor has been found to accompany these changes, the major fraction of the infiltrating cells being neutrophils but also including mast cells and macrophages (9, 12). Experimental depletion of neutrophils through the use of anti-GR1 monoclonal antibodies (mAbs) decreased the tumor response to Photofrin-PDT (Axcan Pharma, Birmingham, AL; Refs. 9, 11, 17). On the basis of these studies, it has become widely accepted that activated neutrophils in the treated tumor play an important role in achieving long-term suppression of tumor growth following PDT.

Several critical inflammatory mediators, such as IL-6 (15), are regulated by redox-dependent transcription factors (18). Therefore, fluence rate, through its control of tumor oxygenation, may influence the generation of inflammatory mediators. Moreover, fluence rate influences PDT-induced vascular changes that are involved prominently in the inflammatory response (19, 20). On the basis of these premises we have hypothesized that the fluence rate used in PDT light delivery will influence the inflammatory milieu generated within the tumor following treatment. We present important evidence that fluence rate not only determines tumor oxygenation during PDT but also that it greatly influences the local inflammatory response that follows PDT exposure. Our studies also reveal that the degree of local inflammation does not always correlate with PDT dose and/or the degree of tumor response and that a strong local inflammatory response can contribute significantly to PDT outcome. They also show that fluence rate can be used to accentuate different components of the spectrum of mechanisms that lead to PDT tumor destruction.

MATERIALS AND METHODS

Animals and Tumor System. Pathogen-free BALB/cJ mice were obtained from The Jackson Laboratory (Bar Harbor, ME). Animals were housed in microisolator cages in a laminar flow unit under ambient light. Six- to 12-week-old animals were inoculated intradermally on the right and/or left shoulder with 10^6 Colo 26 (murine colon carcinoma) cells harvested from exponentially growing cultures (21). Tumors were used for experimentation ~10 days after inoculation when they had reached 6–8 mm in diameter. The RPCI Institutional Animal Care and Use Committee approved all of the procedures carried out in this study.

Reagents. Clinical-grade, pyrogen-free 2-[1-hexyloxyethyl]-2-devinyl pyropheophorbide-a (HPPH) was obtained from the Roswell Park Pharmacy

Received 11/14/03; revised 12/23/03; accepted 1/12/04.

Grant support: NIH Grants CA42278 and CA55791. This work uses core facilities supported in part by Roswell Park Cancer Institute's National Cancer Institute-funded Cancer Center Support Grant CA16056.

The costs of publication of this article were defrayed in part by the payment of page charges. This article must therefore be hereby marked *advertisement* in accordance with 18 U.S.C. Section 1734 solely to indicate this fact.

Requests for reprints: Barbara W. Henderson, Photodynamic Therapy Center, Roswell Park Cancer Institute, Elm & Carlton Streets, Buffalo, NY 14263. Phone: 716-845-4429; Fax: 716-845-8920; E-mail: barbara.henderson@roswellpark.org.

(Buffalo, NY) and reconstituted to 0.4 mM in pyrogen-free 5% dextrose (D5W; Baxter Corp., Deerfield, IL) containing 2% ethanol and 0.1% Tween. Antibodies to murine IL-6 (goat polyclonal IgG) were purchased from R&D Systems (Minneapolis, MN); rat antimurine GR-1 antibodies were purchased from PharMingen (San Diego, CA). Rat IgG and goat IgG were obtained from Caltag (San Francisco, CA) and used as isotype controls.

***In Vivo* PDT Treatment.** Animals were given i.v. injections via tail vein of 0.4 μmol/kg HPPH, followed 24 h later by illumination. Twenty-four h before light treatment, all of the hair was removed by shaving and depilation with Nair (Carter-Wallace, Inc., New York, NY) from the treatment site and from tumors that served as unilluminated controls. Mice were immobilized in specially designed Plexiglas holders without anesthesia during the course of light delivery. The light source consisted of a dye laser (375; Spectra-Physics, Mountain View, CA) pumped by an argon-ion laser (either 171 or 2080; Spectra-Physics). The dye laser, using DCM dye (Exciton, Dayton, OH), was tuned to 665 nm. Output from the dye laser then was passed through an eight-way beam splitter, and the power of each beam was set individually with Brewster window-type attenuators (22). A spot diameter of 1.1 cm was used for all of the treatments. Four illumination regimens were used: 48 J/cm^2 given at 14 mW/cm^2 (the term "given at" is indicated with "@" in the following text and figures), 128 J/cm^2 @ 14 mW/cm^2, 48 J/cm^2 @ 112 mW/cm^2, and 128 J/cm^2 @ 112 mW/cm^2.

Following PDT, animals were either observed for tumor regrowth or killed and tumors harvested for specific experimental analyses. All of the time points for tumor harvest were measured from the beginning of light treatment. All of the experiments included control untreated animals and animals treated with photosensitizer or light only.

Computer Simulation of $^3O_2$ Distribution during PDT. Computer software (PDT molecular oxygen-depletion model), developed by Henning *et al.* (23), was used to visualize the effects of fluence rate on $^3O_2$ distribution throughout the intercapillary space during PDT. Reaction parameters were as described previously (8), with the exception of HPPH tumor concentration, which was 1.95 μg/g (determined by fluorescence in tumor lysates; Ref. 24).

EF3 Binding. 2-(2-Nitroimidazol-1[*H*]-*N*-(3,3,3-trifluoropropyl)acetamide (EF3; SRI International, Menlo Park, CA) was used to visualize hypoxic regions within PDT-treated and control tumors according to published procedures (5). Briefly, photosensitized animals received EF3 (52 mg/kg) via tail vein injection within 3 min of light exposure, and tumors were harvested 30 min later. Control tumors also were exposed to EF3 for 30 min. Immediately before tumor harvest, animals also received (via orbital plexus) 30 mg/kg Hoechst 33342 (Sigma, St. Louis, MO) to allow visualization of perfused vasculature. Tumors were kept frozen at −70°C until analyzed as described previously.

ELISA. Tumors tissues were processed immediately after harvest as described previously (12). Total protein was determined by the Bio-Rad protein assay (Bio-Rad, Hercules, CA). MIP-1, MIP-2, and IL-6 protein levels in control and treated tumors were determined using ELISA kits specific for each protein, purchased from R&D Systems and used according to the manufacturer's suggestion. The assays were performed in duplicate on samples isolated from three animals.

Flow Cytometry. The cell populations present in Colo 26 tumors before and after PDT were characterized phenotypically through fluorescence-activated cell sorter analysis using panels of mAbs to detect specific cell surface antigens as described previously (12). The mAbs conjugated directly with fluorescein, phycoerythrin, or biotin were used to quantify cells expressing the common leukocyte antigen CD45 (Life Technologies, Rockville, MD), CD4 and CD8 T-cell antigens (PharMingen), CD11b (PharMingen), IA^d (PharMingen), and GR-1 (PharMingen). Appropriate immunoglobulin isotypes were used as controls. For cases in which biotinylated antibodies were used, streptavidin-cychrome (PharMingen) was added as a detection reagent. In some experiments, cells were costained with an antibody specific for IL-6 (PharMingen). Intracellular staining of fixed and permeabilized cells was performed according to the manufacturer's instructions.

For flow cytometric analysis, a two-laser FACStar Plus (Becton-Dickinson, San Jose, CA) flow cytometer was used, operating in UV and at 488 nm. Four colors and light-scattering properties could be resolved using 420/20, 530/30, and 575/30 band-pass filters and a 640 long-pass filter. Data were acquired from 5000 cells, stored in collateral list mode, and analyzed using the WinList processing program (Verity Software House, Inc., Topsham, ME). Results are presented as the average number of cells; at least six animals were analyzed for each treatment group.

Immunohistochemical Analyses. Tumors harvested with overlying and adjacent skin were placed immediately in Tris-buffered zinc fixative [0.1 M Tris HCl buffer (pH 7.4) containing 3.2 mM calcium acetate, 22.8 mM zinc acetate, and 36.7 mM zinc chloride] for 6–18 h, transferred to 70% ethanol, dehydrated, and embedded in paraffin. Sections (5-μm-thick) were stained by routine immunohistochemical methods using peroxidase neutralization (3% aqueous hydrogen peroxide for 20 min, blocking with 0.03% casein in PBS/Tween (0.1%) for 30 min, specific antibodies or isotype controls, horseradish peroxidase-linked intermediates, and diaminobenzidine as substrate for detection). Slides were counterstained with Harris hematoxylin (Poly Scientific, Bayshore, NY).

Apoptosis was detected using the Apoptag Plus Peroxidase *In Situ* Detection Kit (Chemicon International, Inc., Temecula, CA), which labels single- and double-stranded DNA breaks by the terminal deoxynucleotidyl transferase-mediated nick end labeling (TUNEL) method. No protein pretreatment of the sections was performed. The diaminobenzidine incubation was for 1.5 min only.

Mouse CD31 was detected with a rat MAb (IgG2a; PharMingen) at 1:50 dilution in PBS for 60 min at 37°C, followed by biotinylated rabbit antirat IgG (12112D; PharMingen) at 1:100 dilution for 30 min, streptavidin peroxidase (50–242; Zymed, South San Francisco, CA) for 30 min, and diaminobenzidine for 5 min.

Mouse IL-6 was detected with a rat MAb (IgG1; ab7375; Abcam Ltd., Cambridge, United Kingdom) at 5 μg/ml, followed by rabbit antirat IgG (E0468; Dako Cytomation, Carpinteria, CA) at 1:300 dilution for 30 min, and Envision + antirabbit horseradish peroxidase (4011; Dako Cytomation) for 20 min, followed by diaminobenzidine (Dako Cytomation) for 5 min.

Determination of Caspase-3 Activity in Tumors. Tumors (three samples for each time point) were harvested at 1, 4, 8, and 24 h after beginning treatment and kept frozen at −70°C until processing. They then were homogenized in 1 ml of a protein extraction solution (1× lysis buffer with 1 mM DTT, 0.5% NP40 by volume, and 5 μg/ml of aprotinin, leupeptin, and pepstatin). The samples then were spun down, and the supernatant was collected. The amount of protein in each sample was determined by Bio-Rad protein assay. Twenty mg of protein from each sample were assayed for caspase-3 activity using the EnzChek caspase-3 assay from Molecular Probes (Eugene, Oregon). When caspase-3 is present, the substrate used in the assay, z-DEVD-AMC, is cleaved to form 7-amino-4-methylcoumarin, which has a fluorescence peak at 450 nm. This fluorescence peak then was measured with a fluorometer (FluoroMax-2; Jobin-Yvon, Edison, NJ; λ_{ex} = 342 nm; $\Delta\lambda_{em}$ = 400–600 nm). The fluorescence was quantitated by integrating the area under the 450-nm fluorescence peak after subtracting the spectra of z-DEVD-AMC alone.

Neutrophil Depletion. Neutrophil depletion was accomplished using anti-GR-1 antibodies (100 μg/mouse; i.v.) administered 24 h before PDT, immediately after, and 24 h after PDT. Control animals were injected with the appropriate isotype as described previously.

Assessment of Tumor Response. Following treatment, orthogonal diameters of tumors were measured once every 2 days with calipers. The tumor volume, *V*, was calculated with the formula $V = (lw^2/2)$, where *l* is the longest axis of the tumor, and *w* is the axis perpendicular to *l*. The tumors were monitored until they reached a volume >400 mm^3, at which time the mice were killed. Regrowing tumors reached the 400 mm^3 volume within ~8 days. No tumor regrowth was observed later than ~day 50; therefore, animals were considered cured if they remained tumor free for at least 60 days after PDT.

Statistical Evaluation. All of the measured values are presented as mean ± SE. The one-tailed Student's *t* test was used for comparison between groups in all of the experiments except for tumor response determinations, with *P* values of 0.05 representing statistical significance. For tumor response data analysis, hours to event (*i.e.*, to 400 mm^3 tumor volume) were calculated for each animal by linearly interpolating between the times just before and after this volume was reached, using log (tumor volume) for the calculations; both tumor volume and hours-to-event calculations were performed using Excel (Microsoft, Redmond, WA). Tumor responses between groups were compared using the Kaplan-Meier analysis. Briefly, the calculated hours-to-event data for individual animals were entered in a Prism (version 3.0; GraphPad Software, Inc., San Diego, CA) spreadsheet. Prism calculates and graphs event curves (*i.e.*, the fraction of subjects not reaching the events as a function of time) for each group and calculates the group median time to event. Event curves were

compared using the Prism program and the log-rank test, which calculated a two-tailed *P* value testing the null hypothesis that the curves were identical.

RESULTS

Fluence Rate Determines Tumor Oxygenation of Colo 26 Tumors during PDT. Fluence rates that deplete or maintain tumor oxygen levels during PDT light exposure have been determined for a number of preclinical tumor models (murine RIF fibrosarcoma and M2R melanoma), and photosensitizers (Photofrin and bacteriochlorophyll serine; Refs. 6, 8). Because these fluence rates depend on many tumor-specific factors, among them photosensitizer uptake and vascular physiology, it was necessary to establish them for the Colo 26 model and HPPH PDT used in this study. Whereas the fundamental mechanisms of photochemical oxygen depletion are expected to be the same as observed with other photosensitizers, specific dosimetric parameters vary. To facilitate the choice of experimental conditions for the biological endpoints, we used the PDT molecular oxygen-depletion model computer software (8, 23), which is derived from the oxygen consumption model (3, 23). Fig. 1*A* depicts the predicted steady-state distribution of $^3O_2$ as a function of the distance from a capillary during tumor illumination with HPPH-PDT at a range of fluence rates between 3.5 and 224 mW/cm^2. From these initial predictions, it was estimated that a fluence rate of 112 mW/cm^2 should lead to significant oxygen depletion within the tumor, whereas a fluence rate of ≤14 mW/cm^2 should maintain tumor oxygen levels. These predictions then were validated for these two fluence rate conditions. We used the hypoxia marker EF3, the binding of which correlates directly with radiobiologically detectable tumor hypoxia (5). Studies in a murine cell line have shown that EF3 binding is most sensitive at oxygen concentrations of 0.01–1% (5); detection of tumor oxygenation within this range is relevant to PDT because direct cell phototoxicity is reduced by half at oxygen concentrations of <0.5–1% (25). EF3 binding, shown in red (Fig. 1, *B* and *C*), is essentially absent in the tumor illuminated with 14 mW/cm^2 light, whereas it is extensive in the tumor treated with light at 112 mW/cm^2. It has to be noted that the total light dose received by the tumors under these conditions differs by ~8-fold, 14 mW/cm^2 illumination corresponding to 25 J/cm^2 and 112 mW/cm^2 corresponding to 202 J/cm^2. Isodose comparison was not possible because EF3 needs at least 30-min exposure to bind. However, as indicated by Hoechst fluorescence (green), tumor perfusion was largely maintained during both treatment regimens. Therefore, it can be concluded that the predominant mechanism for hypoxia induction was photochemical oxygen depletion and that the high fluence rate PDT would lead to considerable regional protection from PDT damage within the tumor. On the basis of this information, all of the other experiments were carried out using these fluence rates for illumination.

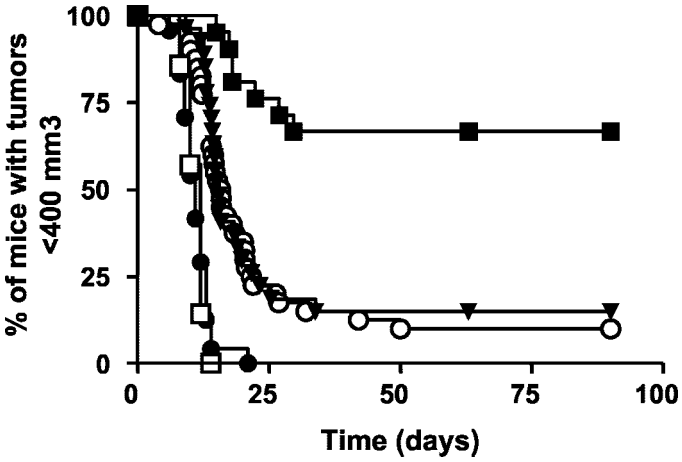

Fig. 2. The photodynamic therapy (PDT) tumor response is fluence and fluence rate dependent. Mice were treated with four different PDT regimens. Tumor growth was monitored for 60 days or until tumors reached a volume of 400 mm^3. Results are reported as the percentage of animals with tumors <400 mm^3. (■) 128 J/cm^2 @ 14 mW/cm^2, $n = 21$; (▼) 128 J/cm^2 @ 112 mW/cm^2, $n = 27$; (○) 48 J/cm^2 @ 14 mW/cm^2, $n = 40$; and (□) 48 J/cm^2 @ 112 mW/cm^2, $n = 7$; (●). Controls, 2-[1-hexyloxyethyl]-2-devinyl pyropheophorbide-a, no light, $n = 24$

The Extent and Characteristics of the Tumor Response Differ with Fluence and Fluence Rate. Earlier work by us and others has demonstrated for several experimental tumor systems that, for a given fluence, low fluence rate light delivery is significantly more efficient than high fluence rate treatment to control tumors by PDT (7, 8). The Kaplan-Meier plots shown in Fig. 2 confirm these observations for the Colo 26 tumor model, the regimen of 128 J/cm^2 @ 14 mW/cm^2 being by far the most effective with ~75% of animals cured. The same light dose delivered at 112 mW/cm^2 produced only ~10% cures. Approximately the same percentage of cures was achieved with only 48 J/cm^2 @ 14 mW/cm^2, whereas that light dose at 112 mW/cm^2 produced no or minimal antitumor effects.

To gain insights into the mechanisms of tissue destruction, we exam-

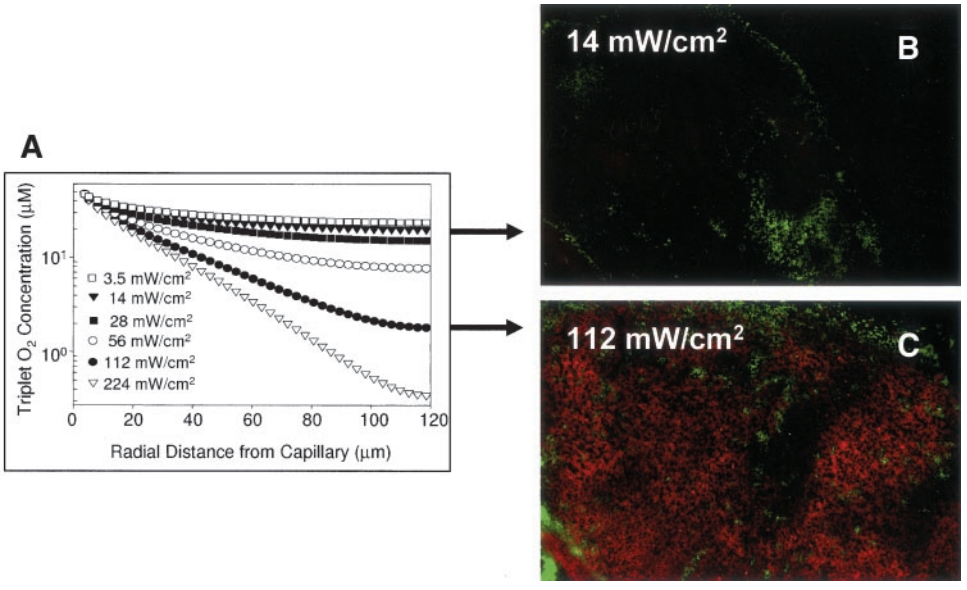

Fig. 1. *A*, simulated ground-state oxygen distribution, plotted by photodynamic therapy (PDT) molecular oxygen-depletion model as a function of the radial distance from a capillary, under different fluence rate conditions (mW/cm^2). *B* and *C*, 2-(2-nitroimidazol-1[*H*]-*N*-(3,3,3-trifluoropropyl)acetamide (EF3) binding (*red*) and perfused vasculature (*green*) in representative sections from Colo 26 tumors exposed to 2-[1-hexyloxyethyl]-2-devinyl pyropheophorbide-a-PDT under different fluence rate conditions. Brighter shades of red indicate more hypoxia, with intensity adjusted for constant camera exposure. EF3 (52 mg/kg) incubation was for 30 min, during which PDT was performed at 14 mW/cm^2 and 112 mW/cm^2; Hoechst 33342 (30 mg/kg) was injected 1.5 min before termination of PDT and tumor excision.

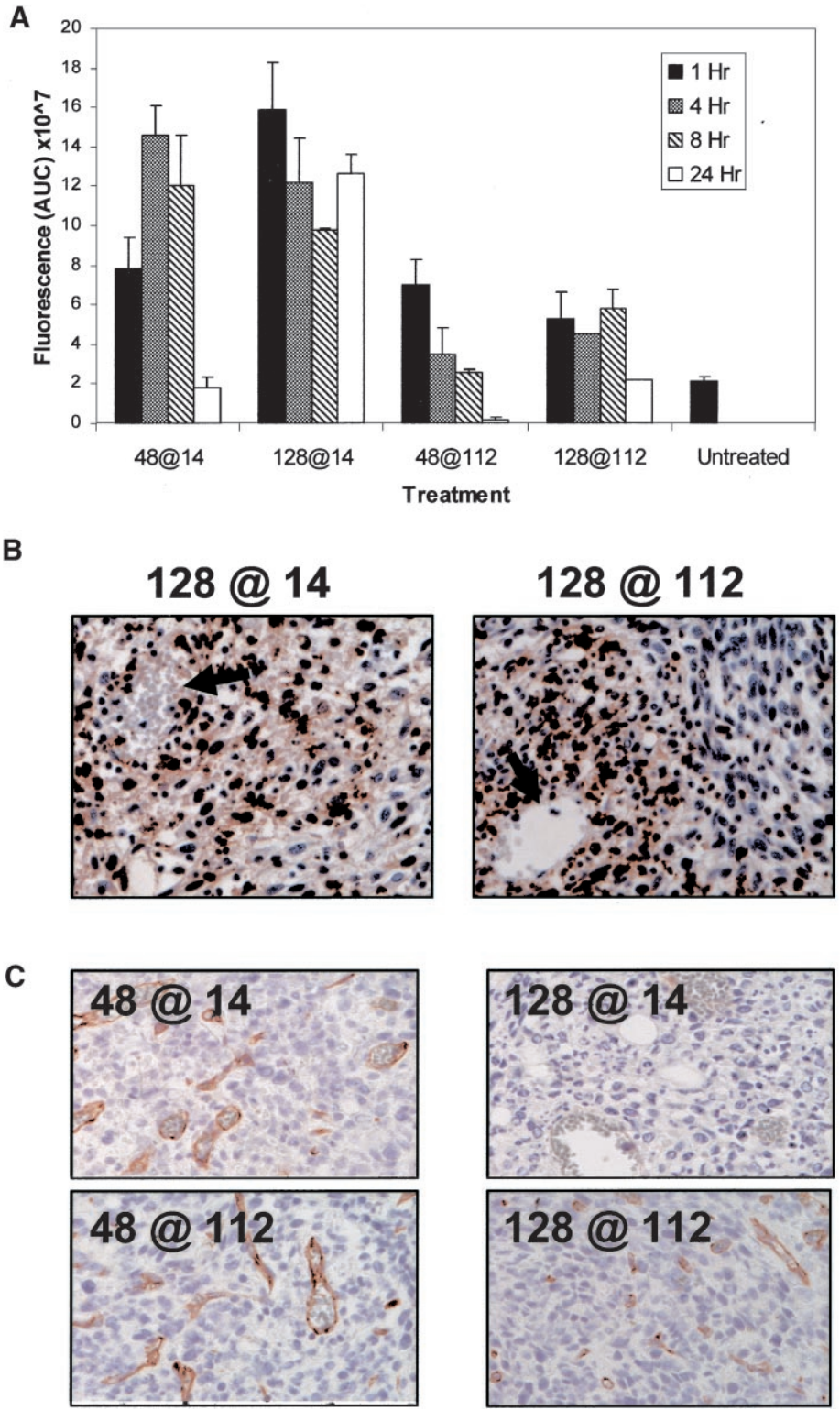

Fig. 3. The extent and character of tumor damage depend on fluence and fluence rate. *A*, caspase-3 activity in protein extracts from tumors as a function of photodynamic therapy (PDT) regimen and time after beginning of illumination. PDT treatment regimens are indicated as J/cm^2 @ mW/cm^2. Data represent the mean ± SE from three mice per point. *B*, terminal deoxynucleotidyl transferase-mediated nick end labeling analysis of tissue sections from tumors harvested 3 h after beginning of illumination. PDT regimens were 128 J/cm^2 @ 14 mW/cm^2 and 128 J/cm^2 @ 112 mW/cm^2; arrows indicate blood vessels; ×400 magnification. *C*, immunohistochemical assessment of the tumor microvasculature. Tumors were harvested 3 h after beginning of illumination with the following PDT regimens: 48 J/cm^2 @ 14 mW/cm^2, 128 J/cm^2 @ 14 mW/cm^2, 48 J/cm^2 @ 112 mW/cm^2, and 128 J/cm^2 @ 112 mW/cm^2; representative tissue sections stained with anti-CD31 and counterstained with Harris hematoxylin are shown; ×400 magnification.

ined apoptotic activity within the tumors by assessing caspase-3 activity in tumor protein extracts as a function of treatment regimen and time after beginning of PDT and by examining tumor sections by TUNEL staining (Fig. 3). HPPH localizes predominantly in mitochondria and PDT cell death with this photosensitizer has the characteristics of apoptosis (26). Enhanced caspase-3 activity, an indicator of apoptotic activity, was observed within 1 h under all of the treatment conditions, but the extent and kinetics of these changes varied (Fig. 3*A*). Note that 1 h into the 128 J/cm^2 @ 14 mW/cm^2 regimen, time intervals being measured from the beginning of light, tumors had received less than half the total dose of 128 J/cm^2. The highest levels of activity were measured for the low fluence rate conditions, with 128 J/cm^2 @ 14 mW/cm^2 reaching the highest levels at 1 h and the most sustained levels at 24 h. Caspase-3 activity in high fluence rate conditions was significantly lower at 4 and 8 h than with

the low fluence rate regimens. In all of the treatment conditions, except 128 J/cm^2 @ 14 mW/cm^2, caspase-3 activity had returned to control levels by 24 h.

The overall lower caspase-3 activity levels observed with high fluence rate PDT can be explained by the distribution of TUNEL positivity in sections from tumors harvested 3 h after beginning of illumination (Fig. 3*B*). Whereas the 14 mW/cm^2 regimen showed TUNEL-positive cells distributed evenly throughout the tumor volume, the 112 mW/cm^2 regimen showed uneven distribution, with TUNEL-positive cells mostly grouped around blood vessels with areas of TUNEL-negative, viable-appearing cells distant from vessels.

To assess the status of the vasculature, we used the panendothelial cell surface marker platelet/endothelial cell adhesion molecule 1 (CD31) to visualize and enumerate blood vessels (Fig. 3*C*). At 3 h after beginning of PDT treatment, CD31-stained blood vessels could be found in tumor samples from all of the treatment regimens. The following values for vessels counted per field (12 fields per tumor) were recorded: control tumors = 6.9 ± 1.93; 48 J/cm^2 @ 112 mW/cm^2 = 9.08 ± 2.20; 128 J/cm^2 @ 112 mW/cm^2 = 8.25 ± 3.17; 48 J/cm^2 @ 14 mW/cm^2 = 7.5 ± 2.0; and 128 J/cm^2 @ 14 mW/cm^2 = 1.5 ± 0.4. Only the last value is significantly different from controls ($P < 0.0001$). In addition to absence of CD31-positive endothelial cells, few morphologically intact endothelial cells could be identified in sections from tumors treated with 128 J/cm^2 @ 14 mW/cm^2.

PDT-Induced Generation of Local Inflammatory Mediators Depends on the PDT Regimen. Having established the appropriate PDT regimens, we proceeded to determine whether/how they might affect the intratumoral generation of inflammatory cytokines and chemokines. IL-6, MIP-1, and MIP-2 were used as indicators of local inflammation, and their levels were measured as a function of PDT regimen in whole tumor protein extracts using ELISA. Expression of these inflammatory mediators has been shown to be up-regulated by PDT *in vitro* (15) and/or *in vivo* (12, 13). Expression of IL-6 was enhanced in PDT-treated tumors under all of the four conditions, but expression levels showed marked and surprising differences among the different treatment regimens (Fig. 4). Under low fluence rate conditions (14 mW/cm^2), 48 J/cm^2 stimulated the highest IL-6 levels, whereas 128 J/cm^2 induced minimal levels of expression (*i.e.*, IL-6 expression exhibited a strong inverse light-dose relationship). Similar patterns were observed for the chemokines MIP-2 and MIP-1, although induction kinetics differed. MIP-2 peaked between 8 and 24 h, whereas MIP-1 levels progressively increased up to at least 48 h after start of PDT. There was a late spike of increased MIP-1 expression at 48 h in the 128 J/cm^2 @ 14 mW/cm^2 regimen. High fluence rate regimens generated low to intermediate expression levels of all of the three indicators and produced the expected light-dose relationship. Light only did not alter the basal chemokine and cytokine profile (data not shown).

PDT Regimen Can Determine the Extent and Distribution of Tumor Infiltration by Inflammatory Cells. Leukocyte migration is a tightly controlled process that is regulated by chemokines and cytokines and mediated by adhesion molecules. Inflammatory neutrophil migration is driven largely by inducible MIP-2 (27), and we have shown previously that neutralization of MIP-2 blocks HPPH-PDT-induced neutrophil infiltration of tumors (13). MIP-1 also participates in neutrophilic inflammation (28). To determine the functional consequences of the different fluence and fluence rate-dependent chemokine expression levels, we assessed tumor infiltration by inflammatory host cells. IL-6 was used as a marker of infiltrating cells for immunohistochemical analysis (Fig. 5, *top*) because its expression was restricted to neutrophils and macrophages, with neutrophils showing the highest expression levels. Examining tumors harvested 3 h after beginning of PDT, marked differences were observed in number and distribution of infiltrating cells. Under 112 mW/cm^2 conditions, 48

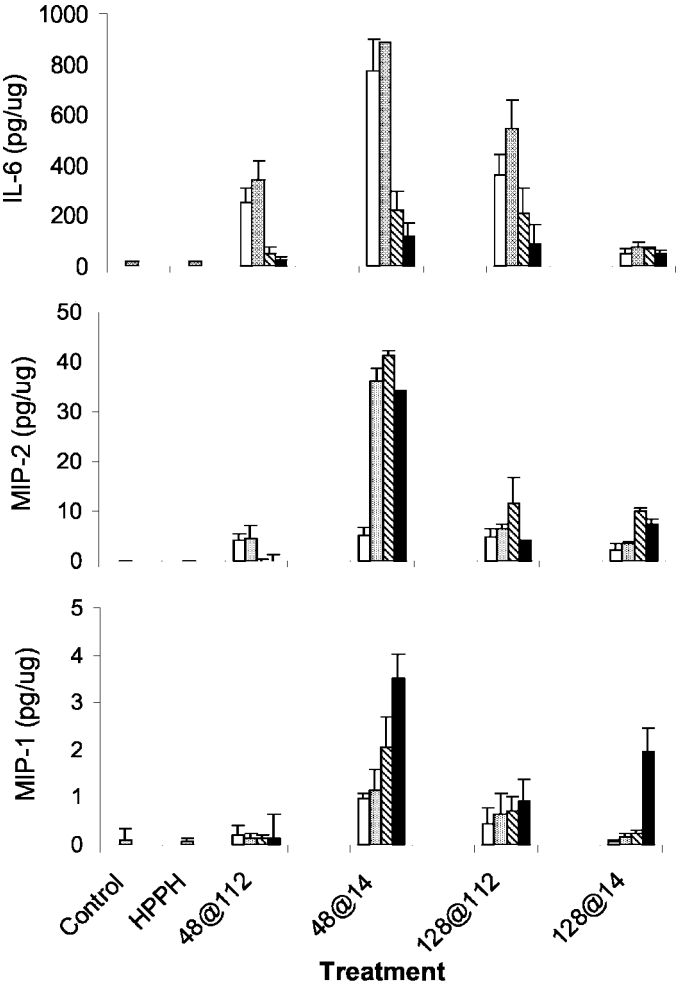

Fig. 4. Induction of interleukin 6 (*IL-6*) and macrophage inflammatory proteins 1 and 2 (*MIP-1* and *MIP-2*) in tumors as a function of time after photodynamic therapy with different treatment regimens. The total amount of protein per sample was determined by Bio-Rad assay (Hercules, CA). IL-6, MIP-2, and MIP-1 levels were determined by ELISA and reported as pg/μg protein. At least three mice were analyzed for each time point, measured from the beginning of light exposure. Error bars represent the SE. (□) 4 h, (▨) 8 h, (▧) 24 h, and (■) 48 h.

J/cm^2 generated minimal numbers of IL-6-positive cells. Larger numbers of such host cells were found with 128 J/cm^2, and these were situated prominently within and around blood vessels. In contrast, 48 J/cm^2 at 14 mW/cm^2 regimens produced substantial diffuse infiltrates that encompassed the entire tumor. Consistent with the minimal expression of inflammatory chemokines under the 128 J/cm^2 at 14 mW/cm^2 regimen (Fig. 4), minimal numbers of infiltrating host cells were observed with that regimen. Flow cytometric analysis of GR-1, CD11b, and IL-6 coexpressing cells, shown in Fig. 5 (*bottom*) for the 24-h time point, again confirms the prominence of the inflammatory infiltrate with low fluence, low fluence rate conditions and the minimal infiltrate for the regimen where the total fluence was increased but fluence rate remained low. These differences remained consistent throughout the 48-h time course of observation (data not shown).

A Strong Local Inflammatory Response Contributes to, but Is Not Critical, for Tumor Control. The contribution of the intratumoral inflammatory response, especially that of neutrophilic infiltrates, to tumor control by PDT has been examined in several previous studies (11, 17). It was found to be significant for various tumor types treated with Photofrin PDT and was believed to be necessary for optimal tumor response. The greatly divergent levels of inflammation and tumor response within the same tumor system

generated by the treatment regimens used here provide an opportunity to examine the correlation, or lack thereof, between tumor response and levels of local inflammation. To accomplish this, we systemically depleted inflammatory neutrophils by administration of anti-GR-1 antibodies and determined the tumor response to treatment with two regimens—48 J/cm^2 @ 14 mW/cm^2 (strong inflammatory cell infiltrate, ~25–30% cures) and 128 J/cm^2 @ 14 mW/cm^2 (minimal inflammatory cell infiltrate, ~75–80% cures). As shown in Fig. 6, elimination of the minimal inflammatory infiltrate observed with 128 J/cm^2 @ 14 mW/cm^2 did not significantly ($P = 0.341$) impair the high cure rates, whereas elimination of the strong inflammatory infiltrate obtained with 48 J/cm^2 @ 14 mW/cm^2 almost completely abolished ($P = 0.008$) the already low cure rates. Depletion of GR-1$^+$ cells was confirmed by flow cytometry analysis, which demonstrated an absence of neutrophils following antibody treatment (data not shown).

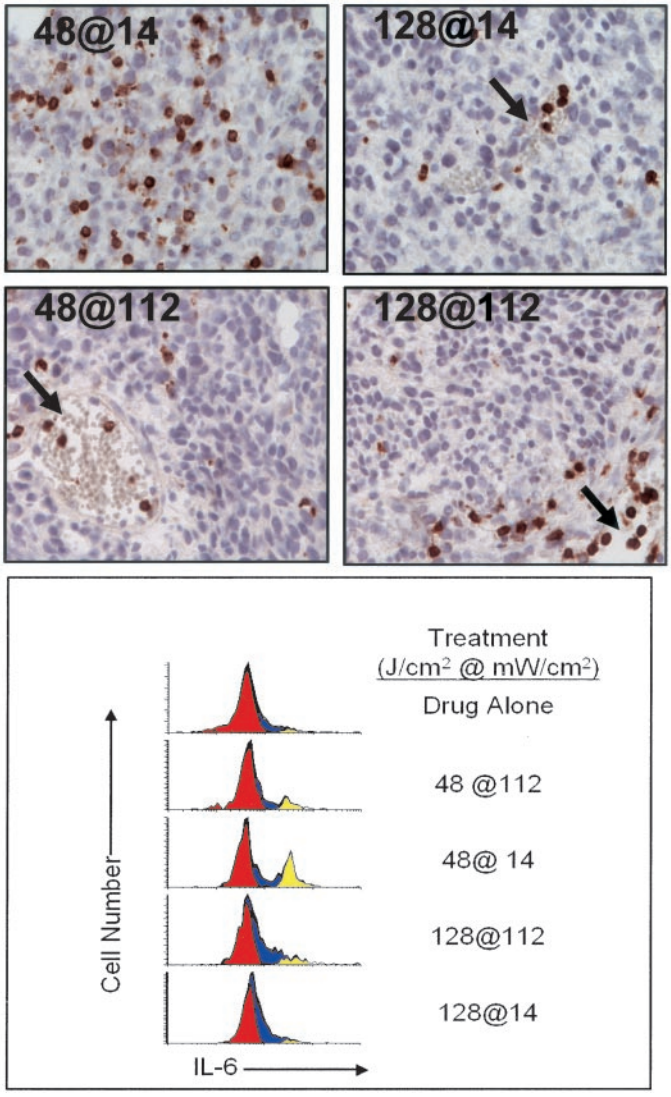

Fig. 5. Tumor infiltration by interleukin 6 (IL-6) expressing inflammatory host cells depends on the photodynamic therapy (PDT) treatment regimen. *Top*, representative sections of tumors harvested 3 h after beginning of light exposure. Sections were stained with anti-IL-6 antibody and counterstained with Harris hematoxylin, ×400. Arrows indicate blood vessels. *Bottom*, representative histograms of intracellular IL-6 expression in tumor-infiltrating leukocytes. *Red*, represents the isotype control staining; *blue*, represents IL-6 expression in GR-1^{lo}, CD11b$^+$ cells (macrophages); and *yellow*, IL-6 expression in GR-1^{hi}, CD11b$^+$ cells (neutrophils).

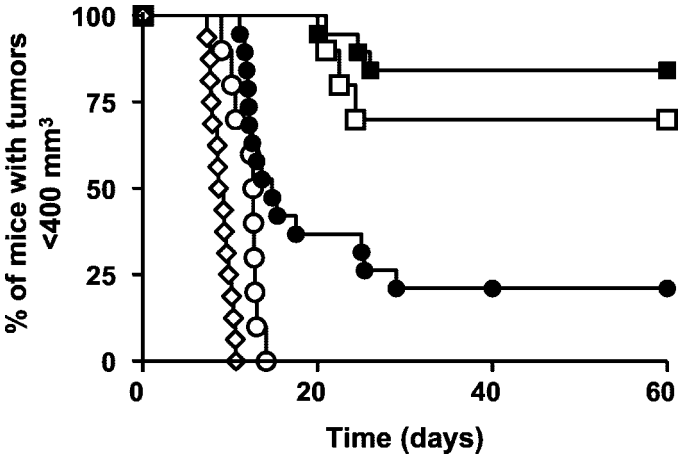

Fig. 6. Depletion of inflammatory neutrophils affects the photodynamic therapy (PDT) tumor response in a PDT regimen-dependent manner. Preceding PDT mice were injected with anti-GR-1 antibody, the appropriate isotype, or saline. Following PDT with two different regimens, tumor growth was monitored for 60 days or until tumors reached a volume of 400 mm^3. Results from control groups have been pooled for simplicity. (■) 128 J/cm^2 @ 14 mW/cm^2 and isotype controls, pooled ($n = 19$); (□) anti-GR-1 antibody +128 J/cm^2 @ 14 mW/cm^2 ($n = 10$); (●) 48J/cm^2 @ 14 mW/cm^2 and isotype controls, pooled ($n = 19$); (○) anti-GR-1 antibody +48 J/cm^2 @ 14 mW/cm^2 ($n = 10$); and (◇) controls: 2-[1-hexyloxyethyl]-2-devinyl pyropheophorbide-a only, anti-GR-1 antibody only, isotype only, pooled ($n = 5$ each).

DISCUSSION

This article addresses three questions of major importance to the management of solid tumors by PDT: (*a*) does the manner in which PDT is delivered affect the local inflammatory response; (*b*) does the local inflammatory response matter for PDT outcome; and (*c*) can the PDT regimen be tailored to achieve optimal treatment conditions, and what are they?

Fluence rate can influence significantly the PDT response of tumors and can be adjusted during PDT treatment, thus potentially allowing the tailoring of treatment to specific lesions and situations (7, 8). Therefore, it is of great importance to understand the mechanisms by which fluence rate affects the PDT response. High fluence rate can result in depletion of tumor oxygen, thereby reducing the primary cytotoxic processes of PDT and affecting tumor control. However, PDT tumor control also appears to be aided by secondary mechanisms, such as microvascular destruction and inflammatory and immune responses. It is reasonable to hypothesize that the elaboration of danger signals, which emanate from PDT tissue damage and set in motion the inflammatory and immune response, will be affected by fluence rate. One additionally would hypothesize that oxygen-conserving low fluence rate PDT, which is known to reach larger tumor volumes than oxygen-consuming high fluence rate PDT and thus produce more extensive tissue damage, would result in a more intense local inflammatory response. In this report, we demonstrate that fluence rate has profound effects on the intratumoral inflammatory response, validating our initial hypothesis. However, the data contradict the second hypothesis because maximum tumor destruction did not correlate with maximum inflammatory response. In fact, the most tumor-damaging and tumor-controlling PDT regimen (128 J/cm^2 @ 14 mW/cm^2) consistently generated the least intense local inflammatory response, as indicated by the low levels of IL-6, MIP-1, MIP-2, and the minimal inflammatory infiltrates. This finding can be explained by the rapid (massive apoptosis occurred within the first hour of PDT) and all-encompassing tissue damage, which would not allow time for cellular up-regulation of inflammatory cytokines and chemokines and would have kept inflammatory cells from entering the tumor. This situation is in contrast to the low fluence delivered at low

fluence rate (48 J/cm^2 @ 14 mW/cm^2); this regimen, while also causing diffuse tumor damage, allowed more tumor elements, including the microvasculature, to survive for longer periods. Surviving cells exposed to sublethal PDT then were able to greatly increase their expression of inflammatory mediators (IL-6, MIP-1, and MIP-2), and the maintenance of the microvasculature enabled host cells to infiltrate the tumor. As expected, high fluence rate conditions protected large tumor regions from PDT damage through oxygen depletion, resulting in considerable heterogeneity in damage and distribution of infiltrating host cells. This is best illustrated in Fig. 3 and Fig. 5, which show IL-6 producing host cells and TUNEL-positive cells present around tumor vessels but absent from undamaged regions distant from the vessels. Unexpectedly, a fluence of 128 J/cm^2 @ 112 mW/cm^2 preserved the vascular endothelium, at least up to 3 h after treatment, whereas the endothelium was obliterated almost completely at that time point when the same fluence was delivered at 14 mW/cm^2 (Fig. 3*C*). This implies that high fluence rate-induced oxygen depletion cannot only occur distant from the microvasculature but also within it. This endothelial protection apparently was temporary and/or incomplete because extensive vascular damage was observed under all of the conditions by 24 h after treatment (data not shown).

The present work confirms previous reports of increased tumor control efficiency of low fluence rate PDT (7, 29). In the Colo 26 model, an 8-fold increase in fluence rate required an ~3-fold increase in fluence to produce equal antitumor effects. These relationships, although extendable to other tumor models, depend on the specific tumor physiology; for equal tumor control of the RIF tumor, for example, an ~15-fold increase in fluence rate requires an ~2-fold increase in fluence (19). It is assumed that the additional fluence mainly is required to photobleach the photosensitizer, thus lowering the rate of $^1O_2$ generation and oxygen depletion. The TUNEL analysis clearly shows the protection of tumor regions distant from microvessels under high fluence rate conditions, supporting the contention that the major parameter influencing treatment outcome is the oxygenation status of the tumor during PDT. Given the fact that under the most oxygen-conserving regimen intratumoral inflammation was minimal and its elimination did not significantly alter the results, it is clear that the optimal oxygen-conserving light dosimetry was the overriding factor responsible for the excellent treatment outcome. This finding challenges previous views that local inflammation is critical to optimal PDT tumor response (1). More accurately stated, it appears that a strong intratumoral inflammatory response is critical under treatment conditions that are suboptimal in terms of oxygen conservation and tumor control. This statement is supported by the observation that elimination of neutrophils from the intense inflammatory response associated with the suboptimal low fluence/low fluence rate treatment virtually abolished tumor control. Lacking at present a clinically usable method to assess directly the status of oxygenation of patients' tumors during PDT, most clinical treatments are likely to fall into the suboptimal category.

Although this work clarifies some of the questions about the role of inflammation in local tumor control, it does not address the possible implications of the intratumoral inflammatory response in control of distant disease. Because inflammation acts as a priming event for the adaptive immune response, the degree of inflammatory changes in the tumor milieu may well influence the generation of an antitumor immune response and potentially affect distant tumor growth. Studies exploring this question are underway.

In summary, we show that (*a*) the intratumoral inflammatory response can be highly fluence and fluence rate dependent; (*b*) that a strong inflammatory response is not critical but can significantly contribute to tumor control; and (*c*) that by adjusting the light dosimetry one can, at least in preclinical systems, shift PDT mechanisms to optimize the direct photodynamic cell kill or to maximally enhance the generation of an inflammatory response.

ACKNOWLEDGMENTS

We thank Ms. Lurine Vaughan and Ms. Barbara Owczarczak for excellent technical assistance.

REFERENCES

1. Dougherty TJ, Gomer CJ, Henderson BW, et al. Photodynamic therapy. J Natl Cancer Inst 1998;90:889–905.
2. Sibata CH, Colussi VC, Oleinick NL, Kinsella TJ. Photodynamic therapy in oncology. Expert Opin Pharmacother 2001;2:917–27.
3. Foster TH, Gao L. Dosimetry in photodynamic therapy: oxygen and the critical importance of capillary density. Radiat Res 1992;130:379–83.
4. Henderson BW, Busch TM, Vaughan LA, et al. Photofrin photodynamic therapy can significantly deplete or preserve oxygenation in human basal cell carcinomas during treatment, depending on fluence rate. Cancer Res 2000;60:525–9.
5. Busch TM, Hahn SM, Evans SM, Koch CJ. Depletion of tumor oxygenation during photodynamic therapy: detection by the hypoxia marker EF3. Cancer Res 2000;60:2636–42.
6. Zilberstein J, Bromberg A, Frantz A, et al. Light-dependent oxygen consumption in bacteriochlorophyll-serine-treated melanoma tumors: on-line determination using a tissue-inserted oxygen microsensor. Photochem Photobiol 1997;65:1012–9.
7. Gibson SL, VanDerMeid KR, Murant RS, Raubertas RF, Hilf R. Effects of various photoradiation regimens on the antitumor efficacy of photodynamic therapy for R3230AC mammary carcinomas. Cancer Res 1990;50:7236–41.
8. Sitnik TM, Hampton JA, Henderson BW. Reduction of tumor oxygenation during and after photodynamic therapy *in vivo*: effects of fluence rate. Br J Cancer 1998;77:1386–94.
9. Korbelik M. Induction of tumor immunity by photodynamic therapy. J Clin Laser Med Surg 1996;14:329–34.
10. Cecic I, Parkins CS, Korbelik M. Induction of systemic neutrophil response in mice by photodynamic therapy of solid tumors. Photochem Photobiol 2001;74:712–20.
11. deVree WJA, Essers MC, DeBruijn HS, Star WM, Koster JF, Sluiter W. Evidence for an important role of neutrophils in the efficacy of photodynamic therapy *in vivo*. Cancer Res 1996;56:2908–11.
12. Gollnick SO, Liu X, Owczarczak B, Musser DA, Henderson BW. Altered expression of interleukin 6 and interleukin 10 as a result of photodynamic therapy *in vivo*. Cancer Res 1997;57:3904–9.
13. Gollnick S, Evans SS, Baumann H, et al. Role of cytokines in photodynamic therapy-induced local and systemic inflammation. Br J Cancer 2003;88:1772–9.
14. Nseyo UO, Whalen RK, Duncan MR, Berman B, Lundahl SL. Urinary cytokines following photodynamic therapy for bladder cancer. A preliminary report. Urology 1990;36:167–71.
15. Kick G, Messer G, Goetz A, Plewig G, Kind P. Photodynamic therapy induces expression of interleukin 6 by activation of AP-1 but not NF-kB DNA binding. Cancer Res 1995;55:2373–9.
16. Evans S, Matthews W, Perry R, Fraker D, Norton J, Pass HI. Effect of photodynamic therapy on tumor necrosis factor production by murine macrophages. J Natl Cancer Inst 1990;82:34–9.
17. Korbelik M, Cecic I. Contribution of myeloid and lymphoid host cells to the curative outcome of mouse sarcoma treatment by photodynamic therapy. Cancer Lett 1999;137:91–8.
18. Yao K-S, Zanthoudakis S, Curran T, O'Dwyer PJ. Activation of AP-1 and of nuclear redox factor, Ref1, in the response of HT29 colon cancer cells to hypoxia. Mol Cell Biol 1994;14:5997–6003.
19. Sitnik T, Henderson BW. The effect of fluence rate on tumor and normal tissue responses to photodynamic therapy. Photochem Photobiol 1998;67:462–6.
20. Henderson BW, Sitnik-Busch TM, Vaughan LA. Potentiation of PDT anti-tumor activity in mice by nitric oxide synthase inhibition is fluence rate dependent. Photochem Photobiol 1999;70:64–71.
21. Henderson BW, Vaughan L, Bellnier DA, vanLeengoed H, Johnson PG, Oseroff AR. Photosensitization of murine tumor, vasculature and skin by 5-aminolevulinic acid-induced porphyrin. Photochem Photobiol 1995;62:780–9.
22. Bellnier DA, Wood LM, Potter WR, Weishaupt KR, Oseroff AR. Design and construction of a light delivery system for photodynamic therapy. Med Phys J 1999;26:1552–8.
23. Henning JP, Fournier RL, Hampton JA. A transient mathematical model of oxygen depletion during photodynamic therapy. Radiat Res 1995;142:221–6.
24. Henderson BW, Bellnier DA, Greco WR, et al. An *in vivo* quantitative structure-activity relationship for a congeneric series of pyropheophorbide derivatives as photosensitizers for photodynamic therapy. Cancer Res 1997;57:4000–7.
25. Chapman JD, Stobbe CC, Arnfield MR, Santus R, Lee J, McPhee MS. Oxygen dependency of tumor cell killing *in vitro* by light-activated Photofrin II. Radiat Res 1991;126:73–9.
26. MacDonald IJ, Morgan J, Bellnier DA, et al. Subcellular localization patterns and their relationship to photodynamic activity of pyropheophorbide-α derivatives. Photochem Photobiol 1999;70:789–97.
27. Biedermann T, Kneilling M, Mailhammer R, et al. Mast cells control neutrophil recruitment during T cell-mediated delayed-type hypersensitivity reactions through tumor necrosis factor and macrophage inflammatory protein 2. J Exp Med 2000;192:1441–51.
28. Adams DH, Lloyd AR. Chemokines: leukocyte recruitment and activation cytokines. Lancet 1997;349:490–5.
29. Sitnik TM, Henderson BW. Effects of fluence rate on cytotoxicity during photodynamic therapy. Thomas J. Dougherty Optical Methods for Tumor Treatment and Detection: Mechanisms and Techniques in Photodynamic Therapy VI. 1997;2972:95–102.